Heliyon 10 (2024) e26945

Contents lists available at ScienceDirect

Heliyon

journal homepage: www.cell.com/heliyon

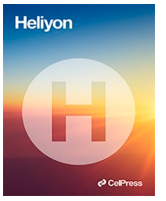

Research article

Comparative analysis of enriched flyash based cement-sand compressed bricks under various curing regimes

Wasim Abbass [a,1], Soheeb Ullah Mahmood [a,1], Ali Ahmed [a], Fahid Aslam [b,*], Abdullah Mohamed [c]

[a] Department of Civil Engineering, University of Engineering and Technology, Lahore, 54890, Pakistan
[b] Department of Civil Engineering, College of Engineering in Alkharj, Prince Sattam bin Abdulaziz University, Al-Kharj, 11942, Saudi Arabia
[c] Research Centre, Future University in Egypt, New Cairo, 11835, Egypt

ARTICLE INFO

Keywords:
Coal fly ash
Fly ash-cement and sand composite bricks
Normal curing
And steam curing

ABSTRACT

This study investigates the substitution of traditional burnt clay bricks (BCB), used since 7000 BCE, with environmentally friendly Fly Ash-Cement and Sand Composite Bricks (FCBs), utilizing industrial waste like Coal Fly Ash (CFA) from thermal power plants. The research encompasses two phases: the first involves experimental production of FCBs, while the second focuses on optimizing FCBs by varying CFA (50%, 60%, 70%), Ordinary Portland Cement (OPC) content (9%–21%), and incorporating stone dust (SD) and fine sand. Comprehensive tests under normal and steam curing conditions, adhering to ASTM C 67-05 standards, include X-Ray Diffraction (XRD), Energy Dispersive X-Ray (EDX), and Scanning Electron Microscopy (SEM) analyses. Results indicate that steam curing enhances early strength, with an optimized mix (MD: 5S) achieving a compressive strength of 15.57 MPa, flexural strength of 0.67 MPa, water absorption rate of 20.08%, and initial rate of water absorption of 4.64 g/min per 30 in^2, devoid of efflorescence. Notably, a 9% OPC and 50% CFA mix (MD: 1S) shows improved early strength of 4.95 MPa at 28 days. However, excessive CFA replacement (70%) with lesser cement content negatively impacts physio-mechanical properties. This research underscores the potential of FCBs as a sustainable and economically viable alternative to BCBs in the construction industry.

1. Introduction

Conventional clay bricks hold a prominent position in Pakistan's construction industry, finding extensive use in residential housing, apartment complexes, and as partition walls within frame structures. Unfortunately, there are growing health concerns among the workers in brick kiln factories. Prolonged exposure to the smoke and dust emitted from these kilns has severely impacted the respiratory health of many laborers [1]. As of April 2018, Pakistan boasted a total of 20,000 operational brick kilns across both rural and urban areas, emitting a range of harmful gases, including CO_2, SO_2, CO, and NO_x [2]. Recognizing the detrimental emissions from these kilns, the Government of Punjab, Pakistan, has taken measures to ban conventional brick kilns in favor of adopting zigzag firing (induced) brick kiln technology. This shift in policy aims to mitigate the adverse environmental effects [2]. According to survey data, Pakistan's annual brick production stands at approximately 82.5 billion bricks, while the demand for baked clay bricks (BCB) is around

* Corresponding author.
E-mail address: f.aslam@psau.edu.sa (F. Aslam).
[1] Joint Author.

https://doi.org/10.1016/j.heliyon.2024.e26945
Received 7 December 2023; Received in revised form 21 February 2024; Accepted 21 February 2024
Available online 24 February 2024

112 billion annually [3]. To address the environmental impact of traditional brick manufacturing, it is imperative to explore alternative resources that support sustainability and environmentally friendly product development.

Coal fly ash is consumed by thermal power plants and in the construction industry, which poses serious environmental problems [4]. It causes air, soil, and water pollution and poses dangers to the ecological cycle. The removal of such waste is a matter of great importance from a conservation perspective [5]. As per the Economic Survey of Pakistan 2021–22, the overall electricity generation from coal power plants is around 5280 MW [6]. A total of 160 million tons of coal fly ash is produced annually. Fly Ash is a natural pozzolanic material that contains aluminates and amorphous irregular silicates [7]. Micro-morphological characteristics of fly ash reveal that it consists of solid spheres, cenospheres, irregularly shaped debris, and porous unburnt carbon [8]. The chemical reactions of fly ash-cement composite involve cement hydration (OPC + Water => C–S–H + CaO) and pozzolanic reaction involves (FA + CaO + Water => C–S–H) which also reduces efflorescence due to the utilization of free lime [9]. The common trend presented in the literature shows the reduction in compressive strength with the existence of CFA in brick earth [10].

Various authors have studied the effect of partial replacement of locally available coal ashes. A study on the utilization of olive-pomace bottom ash in the range of 20–50 % as a replacement for clay. It concluded that an increased percentage replacement of OPBA results in higher water absorption, and lower compressive strength due to porosity [11]. It has been reported that partial replacement by low-volume fly ash (LVFA) may lead to a decrease in compressive strength and increased water absorption [12]. However, studies also report the opposite of this condition which makes it important to study the impact of the addition of fly ash on water absorption [13]. Qazi A. U. et al. studied the development of unburnt coal ash bricks with varying contents of cement (5, 10, 15 wt %), sand contents (10 & 15 wt %), quarry dust contents (5 & 10 wt %) with an applied forming pressure of 29 MPa with moist curing for 28 days. Test results indicated the highest CS value of 19 MPa with (10:60:10:10) and FS value of 2.1 MPa [14]. In literature, frequent research is available on the effect of pressure-temperature-time of fly-based geopolymer ashes, Ahmad M. et al. (2022) studied an individual and combined effect of pressure-temperature-time of geopolymer fly ash-based brick. It summarized that the denser product under molding pressure results in decreased porosity, water absorption, and increased compressive strength. Moreover, hot curing developed better results than ambient curing conditions [15], yet the fact is to explore the behavior of high volume replacement of CFA under ambient conditions and steam curing especially.

Steam curing is a heat treatment method characterized by elevated moisture levels, which expedite the process of cement hydration. The rate of cement hydration demonstrates an augmentation in response to elevated temperatures and longer curing periods [16]. However, it should be noted that excessively high temperatures, particularly in combination with elevated atmospheric pressure, can lead to an undesirable increase in the crystalline structure and quantity of hydrates such as $Ca(OH)_2$ and α-C_2SH crystals. This can result in a weakened structure and compromised bond strength. To optimize the microstructure of the final product, it is essential to mitigate the presence of $Ca(OH)_2$ and α-C_2SH [17]. Steam curing typically operates within a temperature range of 65 °C to 80 °C, with an ideal curing duration of 6 h in a steam autoclave [18]. The temperature level significantly influences both early and late strength characteristics. Higher initial temperatures tend to reduce ultimate strength due to the non-uniform distribution of hydration products, caused by rapid initial hydration resulting from larger capillary pore sizes. Lower temperature curing, although requiring a longer duration, generally yields superior ultimate strength. However, it's worth noting that curing at very high temperatures (up to 100 °C) may lead to deformation when the product is subsequently exposed to normal room temperature conditions, a phenomenon known as delayed ettringite formation. The curing process for masonry products subjected to steam curing typically involves multiple stages to enhance strength development. Allowing the product to remain at room temperature for a period is essential for initial hydration, which improves stability and ultimate strength. The amorphous structure of the hardened product, namely C–S–H, remains consistent, but its composition changes as temperature increases. The specific chemistry of hydration is dependent on the materials used and the curing temperatures. Under normal temperature and atmospheric pressure conditions, Ordinary Portland Cement (OPC) produces C–S–H and CH as hydration products. However, at elevated temperatures and pressure, it undergoes conversion into α-C2SH, a crystalline product. This transformation results in reduced solid-phase formation and increased porosity. The addition of silica alters the hydration sequence, promoting the formation of poorly crystalline C–S–H with lower lime content, as compared to the initial normal hydration reaction. This low-lime gel subsequently transforms into another crystalline hydrate known as tobermorite during continuous heating [19].

Maitra et al. conducted a study that observed an increase in the compressive strength (CS) value of a material up to a heating temperature of 250 °C. The structure of Coal Fly Ash (CFA) exhibits a compact behavior up to 350 °C; however, it begins to deteriorate beyond this temperature threshold due to the breakage of calcium silicates and calcium aluminate hydrates [20]. In a separate case study by Tran et al., the impact of steam curing on the mechanical and durability performance of cement paste was analyzed. This study involved varying fly ash percentages (0%, 20%, 35%, and 50% by weight) in a mixture with a water-to-binder ratio (w/b) of 0.28. The results emphasized that optimal steam curing treatment, combined with an appropriate quantity of fly ash in the cement paste, not only achieved the required design strength in the initial stages but also mitigated long-term detrimental effects associated with steam curing. The optimal curing duration, while limiting the CFA value to 50%, was found to be 4 h [21]. Zhen-Shuang et al. investigated sustainable development and assessed the isolated contributions of fly ash, water-to-binder ratio, and fly ash-to-binder ratio. The results highlighted that the 28-day compressive strength (CS) value decreased as the water-to-binder ratio (w/b) increased from 0.3 to 0.42 [22]. Furthermore, the effect of steam curing on concrete incorporating Class C coal ash was examined. It was observed that coal ash could effectively replace up to 70% of the material while maintaining a constant w/b ratio of 0.4. Steam curing improved the initial age strength, although, at later ages, the strength was found to be comparable for both 50% and 60% coal ash incorporation [23].

2. Research significance

This research article extends existing knowledge on steam curing and its impact on Coal Fly Ash (CFA), with a novel emphasis on augmenting early-age strength through comprehensive comparative analysis. The study's distinctive contribution lies in the meticulous optimization of mixture designs, integrating high-volume CFA, tailored Ordinary Portland Cement (OPC) formulations, and precisely measured inclusions of fine aggregates, namely stone dust and fine sand. These components are examined under both conventional normal curing (NC) and advanced steam curing (SC) conditions, with an overarching ambition to devise a sustainable, eco-friendly Fly Ash Cement Sand Composite Brick (FCB) solution.

Building upon prior investigations that leveraged readily available solid waste materials, such as stone dust, as partial cement substitutes, this study not only aims to enhance material homogeneity but also seeks to significantly boost compressive and flexural strengths. This approach not only presents a cost-effective alternative to traditional sand but also aligns with sustainable construction practices. The crux of this research is an in-depth exploration of varying curing regimes, with a special focus on elucidating the benefits and broader implications of steam curing, thereby contributing valuable insights to the field of sustainable construction materials [24,25]. The current research work aimed at utilizing high-volume fly ash under different curing regimes with different mixture compositions for the production of sustainable fly ash cement-based composite bricks.

3. Materials & methods

3.1. Materials

Coal Fly Ash (CFA), a finely divided residue resulting from the combustion of ground or powdered coal transported by flue gases, serves as a vital component in construction material science. As both a cement replacement and a source of silica and alumina, CFA contributes significantly to the material properties of composites [26]. Its incorporation is known to enhance later-age strength, while marginally reducing drying strength and creep. In this study, four distinct test materials were utilized: CFA sourced from a local paper mill industry; Ordinary Portland Cement (OPC) from a local manufacturer; coarse aggregates including stone dust or quarry dust from a local dealer; and fine sand harvested from the Ravi River.

The selected coarse aggregates, obtained from a crushed stone facility that does not recycle its output, mostly end up in landfills. Their inclusion in the mix not only increases homogeneity but also significantly improves the compressive strength (CS) and flexural strength (FS) of the mix. The dwindling availability of natural fine sand necessitates the exploration of partial replacements, among which stone dust has proven effective. Consistent with existing literature, our findings suggest promising results for up to 40% replacement of stone dust [27,28].

Table 1 presents the chemical composition of all four materials used in the study. The key mineral phases in CFA, primarily responsible for the development of mechanical strength in bricks, are hematite and quartz [29]. According to ASTM C-618, the chemical composition of CFA classifies it as Class F, endowing it with pozzolanic characteristics [30]. These properties make CFA an invaluable resource in enhancing the quality and sustainability of construction materials, particularly in regions where the availability of traditional materials is becoming increasingly scarce or environmentally unsustainable. This study aims to leverage these characteristics of CFA to develop advanced construction materials that meet the dual demands of strength and sustainability.

3.2. Methodology

This research study was carried out on three different levels: In the first level, Microstructural analysis of OPC and CFA was carried out through a Scanning Electron Microscope connected with the EDX. The XRD analysis of CFA and OPC was carried out to determine the phase identification of OPC and CFA. The particle size distribution analysis of coarse aggregates comprising stone dust and fine sand was performed in accordance with ASTM C-136 [31] to check the compliance of particle size distribution with applicable specification requirements and to provide data for control production of aggregate particles. The physical and chemical properties of ingredients incorporated in this study provide crucial data for its application in commercial production. In the second level, trial FCB was developed using a fixed mix proportion of materials i.e., cement: fly ash: sand (10:50:40) treated under normal/moist curing for 7d, and afterward, main FCB was cast at a commercial brick manufacturing unit using different replacement ratios of CFA and tailoring

Table 1
Chemical composition of materials.

Chemical analysis of materials				
Element	Fine sand (%)	Coal ash (%)	Cement (%)	Stone dust (%)
CaO	0.75	3.30	60.39	7.02
MgO	0.68	1.10	2.80	6.95
SiO_2	91.85	77.60	20.50	60.61
SO_3	0.03	1.38	2.61	0.98
Al_2O_3	2.40	5.82	5.14	8.04
Fe_2O_3	1.05	2.45	3.48	5.35
L.O.I	2.18	6.08	3.97	9.58

OPC treated with two curing regimes i.e., normal and steam curing. Table 2 shows different mix designs for the main FCB which comprised of group matrices based upon tailoring of CFA dosages (50%, 60% and 70% by weight), the addition of cement contents in each group fixed with dosages (9%, 12 %, 15%, 18 % and 21% by weight), stone dust (37%–8 %) and fine sand (4%–1%) which conforms to the requirements of ASTM C 136-06 in all the mix designs. A total of 60 trial FCB samples and around 1260 main FCB in total were cast out of which 84 main FCB samples for each mix design were experimented. Mechanical tests including compressive strength and flexural strength on trial FCB were performed on the trial FCB at the age of 7d and 28d whereas the same were replicated on the main FCB at the age of 7d, 28d, 56d, and 90d for both curing regimes. Physical test including efflorescence on trial FCB was performed at the age of 7d, 28d whereas the same was replicated on the main FCB at the age of 28d and 90d for both curing regimes and durability tests including water absorption and initial rate of water absorption on trial FCB were performed on the trial FCB at the age of 7d, 28d whereas the same was replicated on the main FCB at the age of 28d and 90d for both curing regimes. Micromorphology and phase identification analysis were evaluated for the main FCB using SEM, EDX, and XRD respectively. Lastly, a cost comparison was drawn between burnt clay brick and the main FCB.

3.3. Manufacturing of trial and main FCB

Press-formed Fly ash-cement-sand composite bricks sized 9" × 4.5" × 3" were manufactured at a commercial casting yard. All the raw materials were weighed before mixing for a fixed proportion of (Cement: Fly Ash: Sand = 10:50:40) and then transferred to 1 1-ton capacity batch mixer. The water-to-binder ratio was fixed at 0.28. Initial dry mixing was carried for 4 min then water was added gradually, and mixing was continued for another 5–10 min. Afterward, a forming pressure of 3 MPa was applied on the filled molds with mixtures, and then vibration was applied for uniform distribution in all directions for 3–5 s. Sixty FCB units were manufactured which were then placed under moist curing for 7d and were later placed in an open-air environment. Relative humidity was >95% and open-air temperature was 23–25 °C.

Similarly, the main FCB was cast for all the above-mentioned 15 different mixture designs; the water binder ratio was kept constant at 0.28. More than 1260 main FCB samples were manufactured in 15 different batches. A forming pressure of 3 MPa and vibration of 3–5 s was applied on the casted samples. Afterward, all the samples were set aside in a separate place for drying. Markings were earmarked to differentiate the samples.

3.4. Curing treatment

Half of the casted samples (630 No.) were moist curing for 7d while the remaining half (630 No.) were transported to the Laboratory for Steam Curing treatment after attaining a pre-steaming or delay period of 12h. The curing tank consists of two electric heating rods made up of nichrome, each having a capacity of 9 KW that consumes electricity of around 6 KWh with three phases. A temperature controller/thermostat is attached with a temperature-measuring rod to maintain a constant temperature of around 80 °C. The total duration of steam curing for a complete curing cycle was fixed for 6h. All the samples were steam-cured in 3 different shifts. Each shift contained 150 to 160 specimens. After steam curing, samples were dried under open-air conditions.

3.5. Testing procedure

The trial FCB (9" × 4.5" × 3") testing procedure comprising compressive strength, flexural strength, water absorption, the initial rate of water absorption, and efflorescence on 30 FCB samples each at the end of 7d and 28d were tested in accordance with ASTM C

Table 2
Mixture design for the development of FCB samples.

Mixture Designs						
Group	MD	Material Proportions				Curing Treatment
		Cement (%)	CFA (%)	Stone Dust (%)	Fine Sand (%)	
I	1	9	50	37	4	NC, SC
	2	12	50	34	4	NC, SC
	3	15	50	32	4	NC, SC
	4	18	50	29	3	NC, SC
	5	21	50	26	3	NC, SC
II	6	9	60	28	3	NC, SC
	7	12	60	25	3	NC, SC
	8	15	60	23	3	NC, SC
	9	18	60	20	2	NC, SC
	10	21	60	17	2	NC, SC
III	11	9	70	19	2	NC, SC
	12	12	70	16	2	NC, SC
	13	15	70	14	2	NC, SC
	14	18	70	11	1	NC, SC
	15	21	70	8	1	NC, SC

67-05 [32].

Full-size main FCB (9" × 4.5" × 3") were manufactured using an automated brick-making machine for commercial production. The testing procedure contains a total of 1260 samples, out of which physical, mechanical, and durability tests were conducted on each set of 630 samples treated with normal and steam curing regimes. To determine the mechanical performance of bricks in compression, a Compressive Strength test was performed on a Denison Compression Testing Machine having a capacity of 300 Ton, and 0.25-ton accuracy was used. For the compressive strength test specimen, five oven-dried half-main FCB specimens were taken each from NC and SC sets and capping of the main FCB was performed with plaster of Paris one day before the test as prescribed in ASTM C 67-05. The thickness of the capping was maintained the same at 1/8 in. The experimental and schematic arrangement is shown as given in Fig. 1 (a, b). The load rate was maintained at 1.0 mm/min. The gross area of each FCB specimen was measured before the test. Results were compared with limits as mentioned in the Pakistan Building Code (PBC)and ASTM C 62-12 [33,34]. The test was performed at the age of 7d, 28d, 56d, and 90d. The following formulae were used to compute the strength and average of five FCB specimens in each case (NC and SC) and an average of five FCB in each case (NC and SC) was reported in MPa:

$$CS = W/A$$

A flexural Strength test was performed on FRESSIA MACROSS having a capacity of 100 Tons as per the procedure given in ASTM C 67-05. Five full-dried FCB specimens each taken from NC and SC sets were frog-filled with cement paste and placed on two roller supports at a prescribed distance with a 25 mm overhang portion at each end. A concentrated uniform load was applied with a steel rod clearing a 175 mm span to establish a three-point test arrangement and results were computed and compared as per the limit value reported by Abbass W. et al. [4]. The experimental and schematic test arrangement is shown in Fig. 1 (c, d). This test was performed at the end of 7d, 28d, 56d and 90d. An average of five FCB in each case (NC and SC) was reported in MPa:

$$FS = 3W\,(l/2 - x)/bd^2$$

Water absorption tests of the five FCB were measured in accordance with ASTM C 67-05. Results were compared with limits as defined in ASTM C 62-12 [34] for severe and moderate weathering conditions and tests were conducted at the end of 28d and 90d both for NC and SC. Dry and prior weighted specimens were submerged in clean water at room temperature for 24 h. Specimens were then

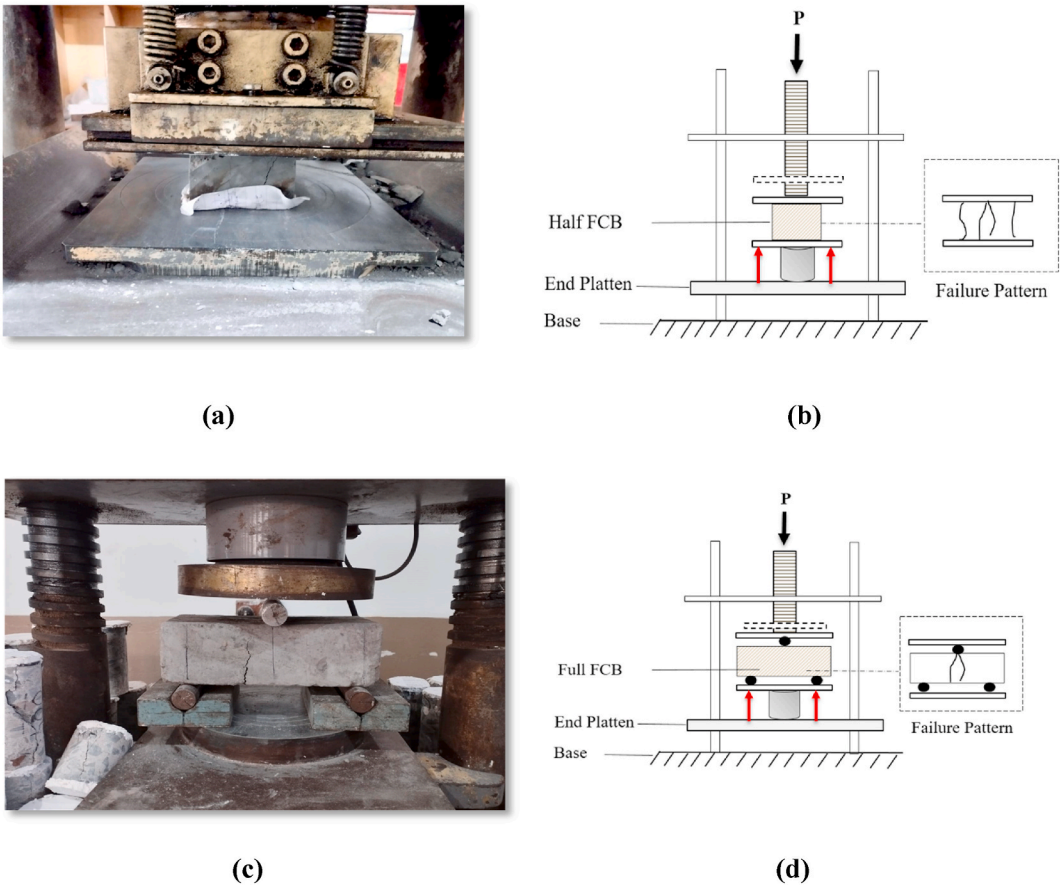

Fig. 1. (a) Experimental setup of flexural strength test, Fig. 1(b) Schematic diagram of compressive strength test, Fig. 1(c) Experimental setup of flexural strength test, Fig. 1(d) Schematic diagram of flexural strength test.

removed from the water wiped off with cloth and then weighed. Average cold water absorption of five FCB in each case (NC and SC) was reported in percentage. The following formulae were used for computations:

$$WA = 100 \times (W_s - W_d) / W_d\ (\%)$$

Similarly, the IRWA test was performed in accordance with the procedure given in the ASTM C-67. Two non-corrodible half-round metal supports attached to a platen were placed inside a container. The water was added up to the top of the supports and the water level was maintained at 1/8 in the above supports. A contact period was maintained for 1 min and water limits were kept within prescribed limits. Specimens were removed after 1 min contact period wiped off with a cloth, and then weighted. The difference between initial and final readings is the amount of water absorbed by the brick during 1 min contact period Results were compared with limit value as reported by Waheed A. et al. [13] and performed at the end of 28d and 90d both for NC and SC. An average of five FCB in each case (NC and SC) was reported in g/min per 30 in^2. The following formulae were used for computations:

$$IRWA = X = 30\ W \,/\, LB\ \left[g \,/\, minper30\ in^2\right]$$

The efflorescence test was performed as per the procedure given in ASTM C-67. Five out of ten allocated FCB were tested each from a set of NC and SC at the end of 28d and 90d. Each FCB was set on end partially immersed and placed vertically in a try; in water to 1 in depth for 7 days in a drying room at a room temperature of 23 ± 2°. Distance between individual specimens was maintained by 2 inches. The second FCB specimen was stored in a drying room without contact with water. Afterward, samples were placed in a drying oven for 24 h. Each pair was examined with normal vision from a distance of 10 ft and based on the appearance and distribution results were reported. An average of five FCB in each case (NC and SC) was reported.

4. Results and discussion

4.1. Particle size distribution analysis

Fig. 2 shows the suitability of stone dust and fine sand for the design of mixtures for fly ash brick production. The particle size distribution analysis showed for control usage of fine aggregates that the controlled percentage cumulative weight retained on #200 for SD was 90% and 10% in the case of fine sand to be used as a proportion of the total mixture. The fineness modulus of fine aggregates was 3.12, which is within acceptable limits as per specified standards.

4.2. Material characterization

Fig. 3 shows the major peaks of quartz, alite, gypsum, belite, and traces of tetra calcium alumina-ferrite and lime similar to research conducted by Abdalla A.A. et al. [35] whereas, in the case of CFA, the major peaks are quartz, lime and minor peaks of hematite. Table 1 indicates the chemical composition of raw ingredients i.e. coal ash, cement, stone dust, and fine sand. The main elements observed in CFA were SiO_2 (77.6 %), Al_2O_3 (5.82%), and Fe_2O_3 (2.45%) and as per chemical requirements of ASTM C 618-12a, the sum of these oxides should be greater than 70 %; maximum contents of SO_3 contents (1.38%) should be 5% and L.O.I (6.08% ≯ 6%) should be 6%. Hence, the coal ash used in this study was classified as Class F. Previous studies indicated that coal ash containing higher L.O.I would require much water due to unburnt carbon fragments [36]. Other requirements of ASTM include CaO content (3.30%) must be less than 18% and that was satisfied. The main elements present in OPC were CaO (60.39%), SiO_2 (20.5%), Al_2O_3 (5.14%) Fe_2O_3 (3.48%), and other alkali elements. These alumina and iron oxides in CFA react with CaO in OPC to form C-A-S-H gel [14] whereas C_3S and C_2S react with water to form C–S–H gel and CH [19] which provides the required strength to mortar mixture. The chemical composition of stone dust and fine sand indicates greater content of SiO_2 (60.61 %, 91.85 % respectively), and L.O.I (9.58%, 2.18%, respectively) which indicates a higher percentage of unburnt carbon particles that are present in stone dust [4].

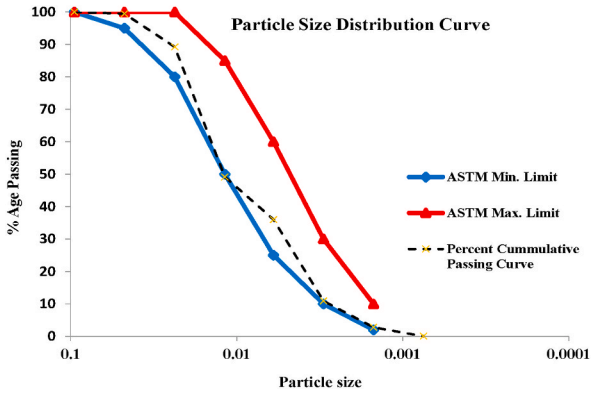

Fig. 2. Particle size distribution of stone dust and fine sand.

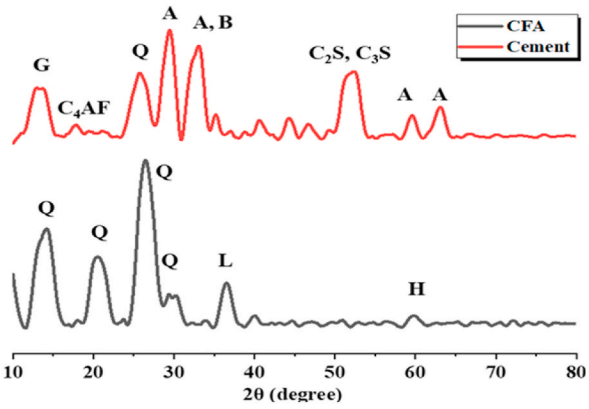

Fig. 3. XRD analysis of OPC, CFA.

4.3. Micromorphology of materials

Fig. 4 shows the micromorphology of OPC and CFA. It showed that OPC contains major particles of Alite and Belite as illustrated by the SEM analysis. The amorphous irregular structure of CFA is likely because of some of the minerals in the coal fly ash which might not undergo a melting phase but soften only under low temperatures of 850-900 °C [8]. Fig. 4 (a, b) shows the combined EDX and SEM results of materials (CFA, OPC) which highlights major peaks of calcium, silicon, carbon, and iron contents. The results so obtained endorsed the chemical composition of materials.

4.4. Physical, mechanical, and durability properties of trial and main FCB

Pilot Study.

Table 3 shows the mechanical, durability, and physical properties of the mixture produced in the pilot study in accordance with ASTM C 67-05. It was observed that trial FCB incorporating higher CFA (50%) content and under ambient curing conditions depicted delayed strength gain at early ages. Moreover, durability properties depicted that optimization of the mixture needs to be carried out in order to achieve accurate behavior as per standard requirements.

4.4.1. Main FCB

4.4.1.1. Compressive strength (influence on addition of OPC, replacement of CFA, and different curing regimes). Fig. 5 depicts the effect of dosage of OPC, replacement of CFA, and curing regimes on the compressive strength (CS) of fly ash bricks. The average results of five FCB under NC and SC cured specimens were assessed at the curing age of 7d, 28d, 56d, and 90d. Table 4 shows the coefficient of variation (CoV) of compressive strength for all the mixture designs, which was less than 10%. It was observed that compressive strength increased with an increase in the addition of OPC keeping the dosage of CFA constant. For instance, the maximum value of 15.57 MPa at 90d was obtained with a 21% addition of OPC and 50 % replacement of coal fly ash (MD:5S) in comparison to 6.71 MPa

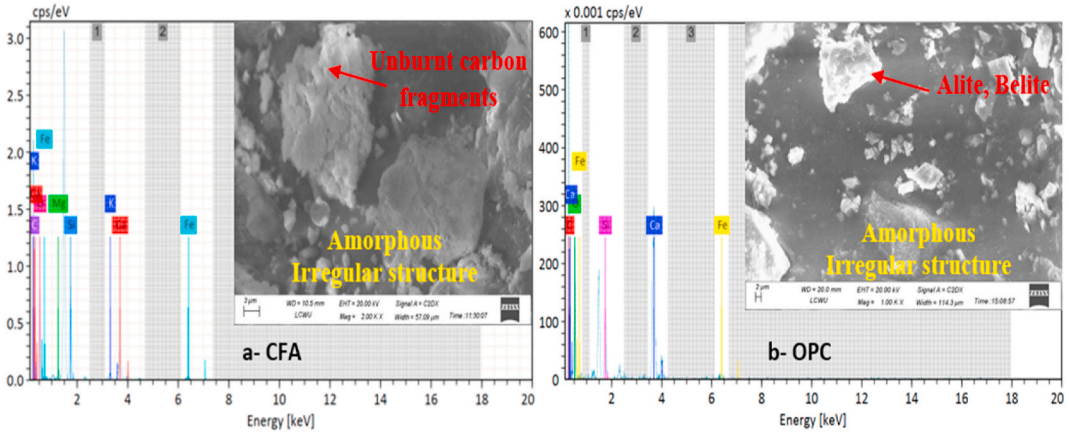

Fig. 4. Sem &energy dispersive X-Ray of (a) CFA and (b) OPC.

Table 3
Test results of pilot study.

Properties	Mechanical Properties		Durability Properties	Physical Properties	
	Compressive Strength (MPa) 7d and 28d	Flexural Strength (MPa) 7d and 28d	Water Absorption (%) 7d and 28d	Initial Rate of Water Absorption (g/min per 30 in^2) 7d and 28d	Efflorescence 7d and 28d
Values	3.5 and 4.0	0.038 and 0.174	19.7 and 21.5	50.4 and 51.1	Nil

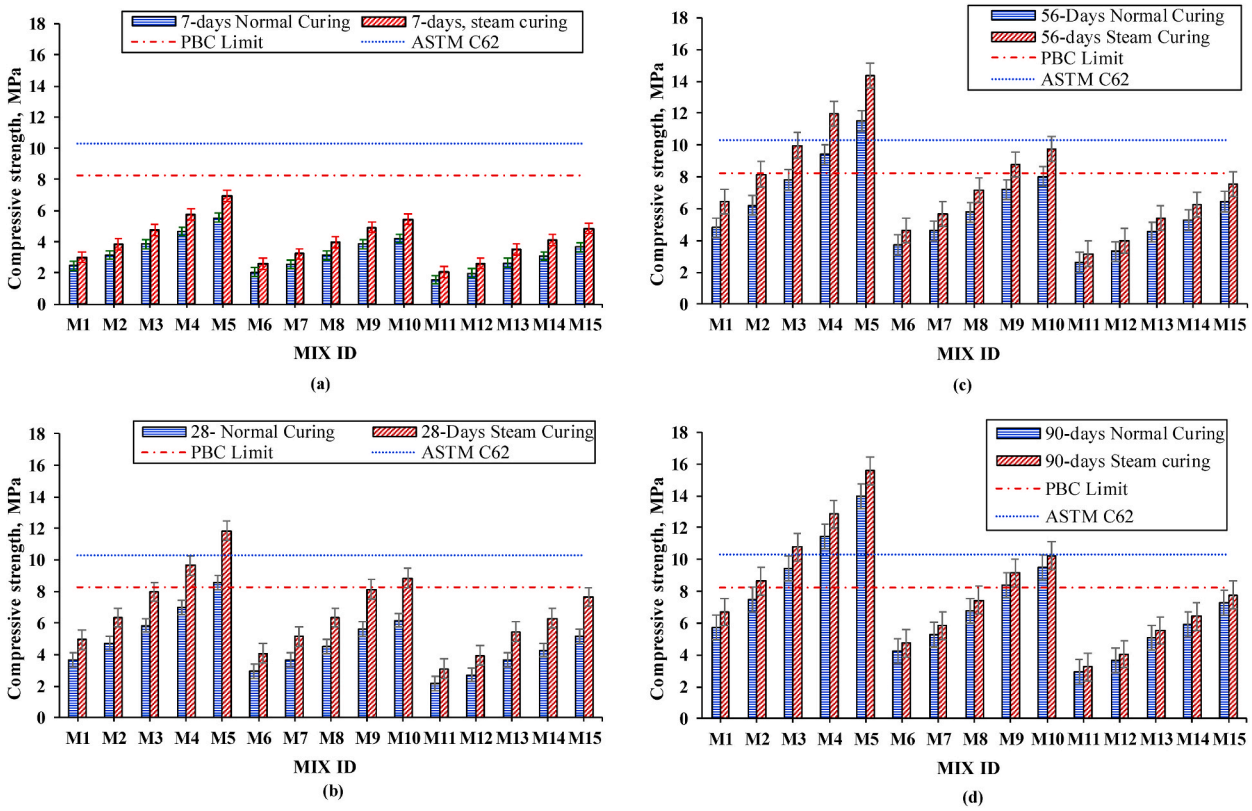

Fig. 5. Compressive Strength of main FCB with different OPC and CFA contents under Normal and Steam Curing regime.

Table 4
Co-efficient of Variation for different design mixes.

Tests	Co-efficient of Variation COV, (%)														
	M1	M2	M3	M4	M5	M6	M7	M8	M9	M10	M11	M12	M13	M14	M15
Compressive Strength	3	5	7	6	2	2	6	5	3	7	6	8	9	9	6
Flexural Strength	4	3	5	7	8	7	9	8	6	3	7	2	5	2	5
Water Absorption	4	5	9	8	6	6	4	9	5	5	1	7	8	9	6
Initial Rate of Water Absorption	0.1	0.4	0.1	0.5	0.2	0.1	0.2	0.1	0.1	0.3	0.1	0.1	0.2	0.7	0.2

at 90d with a 9% addition of OPC and at constant CFA content of 50 % (MD:1S) with a constant water to binder ratio of 0.28. An increase in compressive strength was within the range of 22%–57%; 19%–54% and 20%–58% with OPC addition varying from 12% to 21% (for 2S to 5S; 7S to 10S and 12S to 15S, respectively) as compared to their corresponding first dosages of OPC at 9% (MD: 1S, MD: 6S and MD: 11S). The increase in compressive strength may be attributed to the formation of cement hydration products i.e. C–S–H gel developing from a reaction occurring between tri-calcium silicate (C_3S) and di-calcium silicate (C_2S) with water [4,19]. Further studies also highlighted that the presence of CaO and SiO_2 has a positive impact on the compressive strength of the mixture containing the CFA [35]. Moreover, the compressive strength of the normal-cured specimen followed a similar trend of increase in compressive strength with the addition of cement, however, the compressive strength of normal cured specimen was lesser in comparison to the steam-cured specimen. For example, the percentage increase for normal cured specimens in mixture designs 2 N–5 N; 7 N–10 N, and 12 N–15 N at

90d were 23%–59 %; 20%–55%, and 21–60% as compared to their corresponding first dosages each at 9% (1 N, 6 N and 11 N).

The results also showed that compressive strength decreased with an increase in the replacement of cement with CFA. The replacement of cement with fly ash presented improvement in workability and compressive strength with certain dosages [37]. This was consistent with the available literature [12]. It was also highlighted that under NC and SC regimes, the incorporation of higher CFA leads to a reduction in compressive strength [38]. For instance, a mixture design incorporating 50% replacement of CFA (5S) has shown a maximum value of 15.57 MPa corresponding to the reduced value of 10.2 MPa and 7.8 MPa with replacement of 60% (10S) and 70% (15S). When the replacement of fly ash was low i.e. 50% by weight of cement, the dilution effect passes over the reduction of cement quantity in the binder leading to a higher compressive strength value at the initial stage. However, when the replacement of fly ash in the binder was greater (60% and 70 % by weight), it reduced the quantity of cement in the binder, bringing about a reduction in hydration products [21]. This decrease in compressive strength for steam-cured varies from FCB 29%–34% for 6S to 10S and from 52% to 50% for 11S to 15S as compared to the first dosage at 50 % 1S to 5S. Moreover, the compressive strength of the normal-cured specimen followed a similar trend of a decrease in strength values with an increase in replacement of CFA, however, the values were lesser in comparison to the steam-cured specimen. For instance, the percentage decrease for normal-cured specimens in mixture designs 6 N–10 N; and 11 N–15 N at 90d were 26–32% and 49 to 48% as compared to the first dosage at 50% (1 N–5 N).

Fig. 5 (a, b, c, d) indicates the percentage increase in compressive strength effect in steam-treated samples in all the mixture designs over normal/moist cured samples at all ages. However, this impact was decreasing with higher replacement levels of CFA. At elevated temperatures, a less reactive form of silica also takes part in the pozzolanic reaction, which normally remains inactive; acts as filler material, and causes a reduction in strength [19]. Undesirable α-dicalcium silicate hydrate in the presence of silica at high temperature and pressure converted to tobermorite. This results in a decrease in porosity and, an improvement in bond strength [39,40]. It was also observed that a mixture design incorporating 9% OPC; and 50% CFA (1S) achieved better early strength i.e., 4.95 MPa at 28d

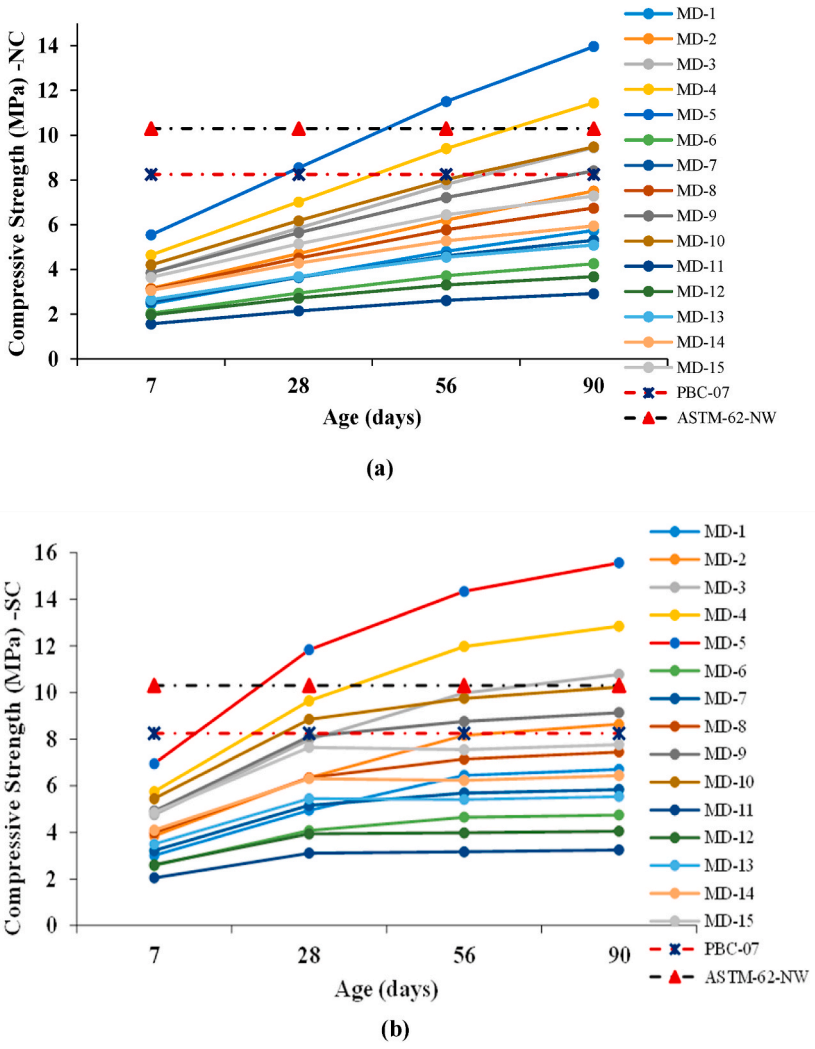

Fig. 6. Compressive Strength varies with the age of the main FCB under different curing regimes.

indicating improved mechanical properties under the influence of steam curing treatment.

Moreover, results of compressive strength involving various quantities of CFA and OPC were compared with limiting values as defined in Pakistan Building Code, 2007 and ASTM C62-12a i.e., 8.25 MPa [33] and 10.3 MPa [34]. The mixture design incorporating 21% OPC and 50% CFA content under steam curing (5S) has satisfied the limiting values of PBC and ASTM C62-12a. Also, a mixture design incorporating 18% OPC, and 50% (4S) has satisfied the limiting value of PBC. Other mixture designs (3S) and (2S) have also satisfied the requirements of ASTM C62-12a and PBC-07, respectively at later ages 90d which confirms that the extended pozzolanic activity occurs due to the presence of silica at high temperatures and as a result, an increased chain length of C–S–H. Likewise, mixture designs 9S and 10S incorporating the 18% and 21% OPC, respectively with a constant 60% CFA content have also satisfied the requirement of PBC-07.

4.4.1.2. Compressive strength with age of FCB sample. Fig. 6 shows the relationship of compressive strength characteristics at the initial and later ages. The results showed that compressive strength in the NC regime does not differ so much (flat curve) since a normal hydration reaction takes place where most of the silica remains inert and acts as filler. On the contrary under the SC regime, the compressive strength increased considerably at the initial stage (sharp curve at 7d & 28d) because the hydration reaction proceeds swiftly due to higher $Ca(OH)_2$ presence at the initial phase while it becomes almost equivalent at later stages (flat curve at 56d and 90d) [41,40]. Overall, an increasing trend of compressive strength in both regimes is due to the long-term effect of CFA on compressive strength, which was greater than the short-term effect [35]. Moreover, the activity of supplementary materials is enhanced due to higher temperatures under steam curing [42]. For instance, the compressive strength of mixture 5 N containing 21% OPC and 50% CFA has a value of 8.55 MPa at 28d compared to 13.97 MPa at 90d. Whereas with the same contents of CFA and OPC under steam curing regime (5S), it was 11.84 MPa and 15.57 MPa at 28d and 90d, respectively. The difference between the two regimes was 28% higher at initial days (28d) whereas that difference reduced to 10% at later ages (90d). The studies revealed that suitable heat curing can enhance the hydration reaction, speed up gel formation, and increase the strength [39]. This also implies that FCB samples under steam curing have a higher rate of gain in strength than FCB under normal cure.

4.4.1.3. Flexural strength (influence on addition of OPC, replacement of CFA, and different curing regimes). Fig. 7 shows the effect of dosage of OPC, replacement of CFA, and curing regimes on the flexural strength (FS). Average results of five FCB under NC and SC cured specimens were assessed at the curing age of 7d, 28d, 56d, and 90d. Table 4 shows the coefficient of variation (CoV) of flexural strength for all the design mixtures was less than 10%. It was observed that flexural strength increased with an increase in the addition of OPC keeping CFA constant. Flexural strength follows a similar trend to compressive strength [22]. For instance, maximum value of

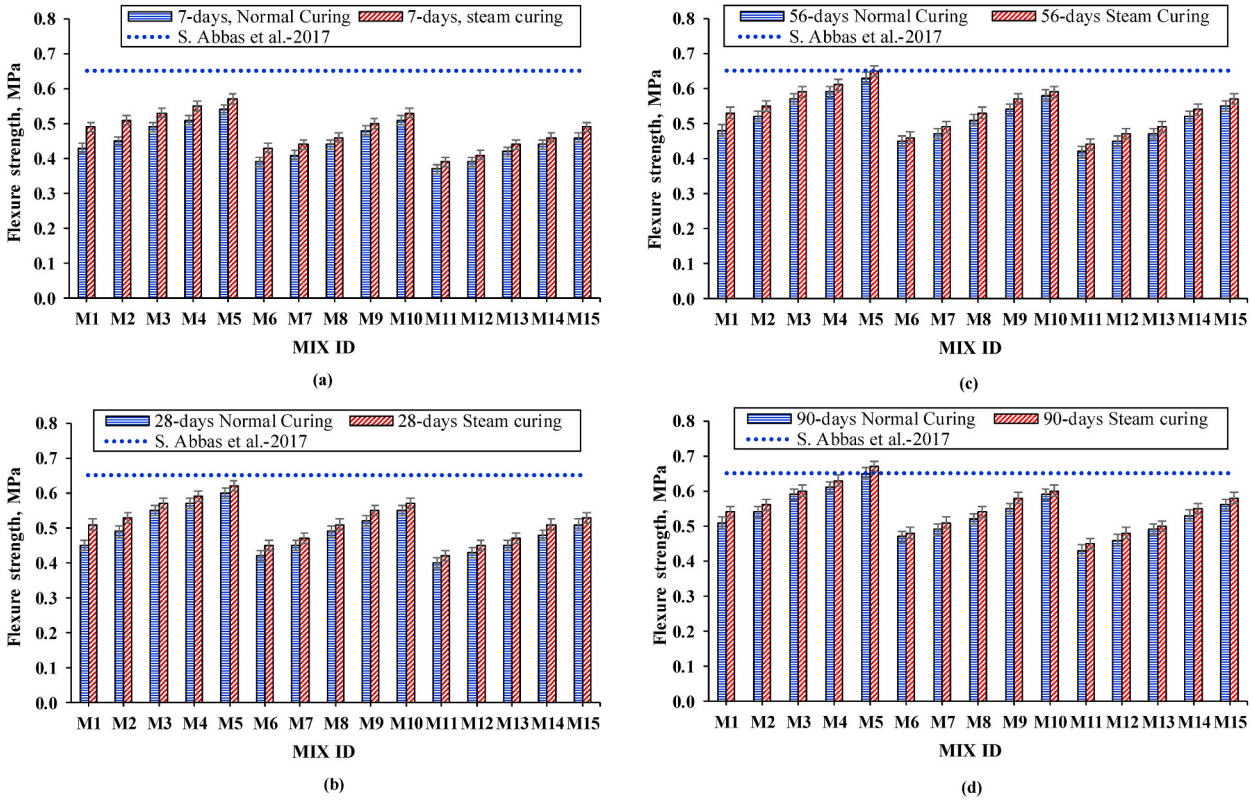

Fig. 7. Flexural Strength of main FCB with different OPC and CFA contents under Normal and Steam Curing Regime.

0.67 MPa at 90d was obtained with 21% addition of OPC and 50 % replacement of coal fly ash (5S) in comparison to 0.54 MPa at 90d with 9% addition of OPC and at constant CFA content of 50 % (1S) with a constant water to binder ratio of 0.28. An increase in flexural strength was within the range of 04%–19%; 06%–20% and 06%–22% (with OPC addition varies at 12%–21%) for 2S to 5S; 7S to 10S and 12S to 15S, respectively as compared to their corresponding first dosages of OPC at 9% (1S, 6S and 11S). The increase in flexural strength might be attributed to the formation of cement hydration products i.e., C–S–H gel developing from a reaction occurring between tri-calcium silicate (C_3S) & di-calcium silicate (C_2S) with water [4,19]. On the contrary, the flexural strength of the normal cured specimen followed a similar trend of increase in strength with the addition of cement, however, the values are lesser in comparison to the steam-cured specimen. For instance, the percentage increase for normal-cured specimens in mix designs 2 N–5 N; 7 N–10 N, and 12 N–15 N at 90d was 06%–22 %; 04%–20%, and 07–23% as compared to the first dosage at 9% (1 N, 6 N and 11 N).

The results showed that flexural strength decreased with an increase in the replacement level of CFA. This was consistent with the available literature [12]. It was noted that under NC and SC regimes, the incorporation of higher dosages of CFA leads to a reduction in FS [38]. Also at a lower water-to-binder ratio (0.28), the degree of reaction decreased with increased dilution of CFA [40]. For instance, a mixture design incorporating 50% replacement of CFA (5S) has shown a maximum value of 0.67 MPa corresponding to the reduced value of 0.6 MPa and 0.58 MPa with replacement of 60% (10S) and 70% (15S). When the replacement of cement with fly ash is low i.e., 50% by weight, the dilution effect passes over the reduction of cement quantity in the binder leading to a higher FS value in the initial stage. However, at a greater replacement level of fly ash (60 & 70 % by wt.), it reduced the quantity of cement in the binder,

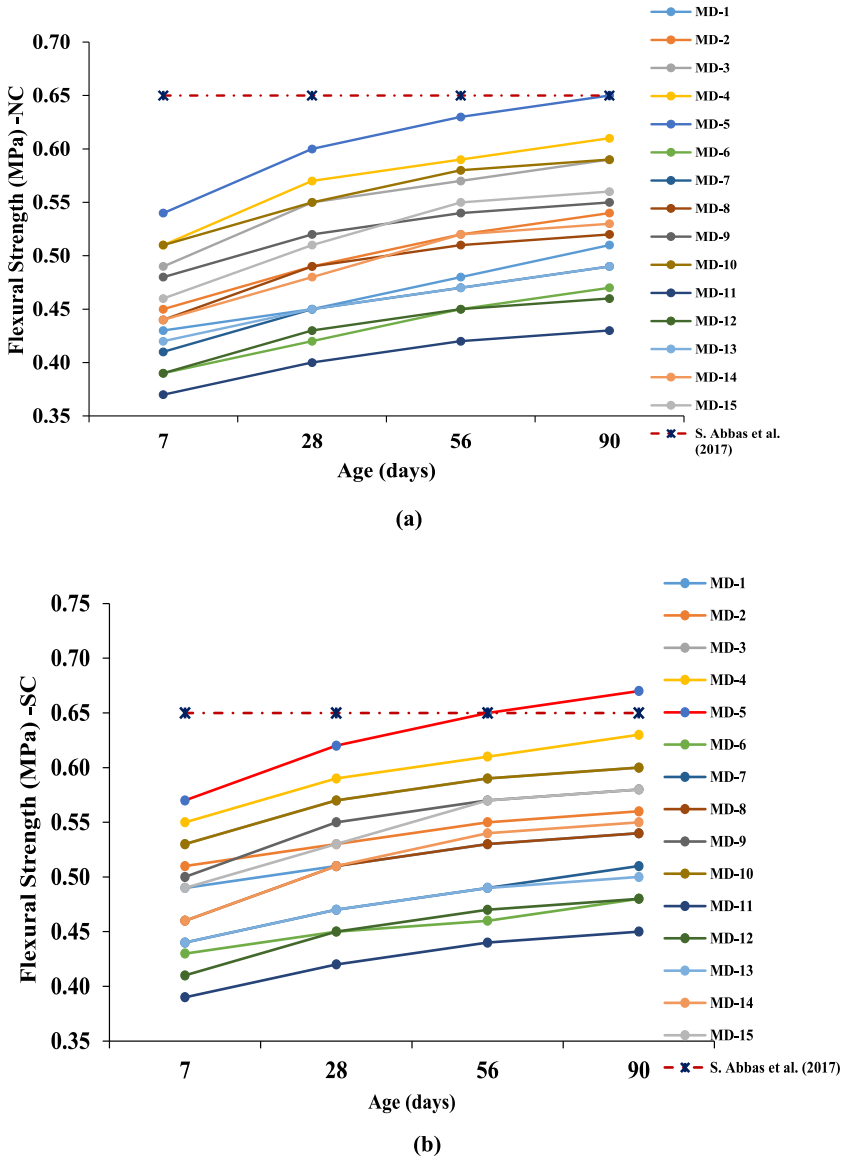

Fig. 8. Flexural strength varies with the age of FCB under different curing regimes.

bringing about a reduction in hydration products [21]. This decrease in FS varies within the range from 11% to 10% for 6S to 10S and from 17% to 13% for 11S to 15S as compared to the first dosage at 50% for 1S to 5S. On the contrary, the flexural strength of normal-cured specimens also followed a similar trend with increased replacement of CFA, however, the values were lesser in comparison to steam-cured specimens. For instance, the percentage decrease for normal cured specimens in mixture designs 6 N–10 N; and 11 N–15 N at 90d was 08%–09 % and 16 to 14% as compared to the first dosage at 50% (1 N–5 N).

Fig. 7 (a, b, c, d) shows the percentage increase in FS in steam-cured samples in all the mixture designs over normal/moist-cured samples at all ages. However, this impact was increasing with higher replacement of CFA. At elevated temperatures, a less reactive form of silica also takes part in the pozzolanic reaction, which normally remains inactive; acts as filler material, and causes a reduction in strength [19,43]. Undesirable α-dicalcium silicate hydrate in the presence of silica at high temperature and pressure converted to tobermorite leading to a decrease in porosity, and improvement in bond strength [38,44]. It was also observed that a mixture design incorporating 9% OPC; and 50% CFA (1S) achieved better early strength i.e., 0.51 MPa at 28d indicating improved mechanical properties under the influence of steam curing treatment.

Moreover, results of flexural strength involving various quantities of CFA and OPC were also compared with the limiting values specified by ASTM C62-12 i.e., 0.65 MPa [4]. The mixture design incorporating 21% OPC and 50% CFA content under treatment with steam curing (5S) has satisfied the minimum specified limits of ASTM C62-12a.

4.4.1.4. Flexural strength with age of FCB sample. Fig. 8 shows the relationship of flexural strength characteristics at the initial and later ages. The results showed that FS values in the NC regime did not differ so much (flat curve) since a normal hydration reaction takes place where most of the silica remains inert and acts as filler. On the contrary, under the SC regime, FS values increased considerably at the initial stage (Sharp curve at 7d and 28d) because the hydration reaction proceeds swiftly with higher $Ca(OH)_2$ presence at the initial phase while it becomes almost equivalent at later stages (flat curve at 56d and 90d) [38,41]. Overall increasing trend of FS in both regimes is due to the long-term effect of CFA on FS, which is greater than the short-term effect [35]. Moreover, the activity of supplementary materials is enhanced due to higher temperatures under steam curing [42]. For instance, the flexural strength of 5 N containing 21% OPC and 50% CFA has a value of 0.6 MPa at 28d compared to 0.65 MPa at 90d. On the other hand, with the same contents of CFA and OPC under a steam curing regime (5S), it was 0.62 MPa and 0.67 MPa at 28d and 90d, respectively. It indicates that the difference between the two regimes is 3.23% higher at initial days (28d) whereas that difference is reduced to 3% at later ages (90d). The studies revealed that suitable heat curing can enhance the hydration reaction, speed up gel formation, and increase strength [39]. It implies that FCB specimens under steam curing have a higher rate of gain in strength than FCB under normal cure.

4.4.1.5. Water absorption (influence on addition of OPC, replacement of CFA, and different curing regimes). Fig. 9 presents the effect of the replacement of CFA and dosage of OPC and curing regimes on water absorption (WA). The average of five FCB specimens under NC and SC cured were assessed at the curing age of 28d and 90d. Table 4 shows the coefficient of variation (CoV) of water absorption for all the design mixes. The CoV was less than 10%. With the increased replacement of OPC, water absorption was reduced in both regimes perhaps due to the formation of C-A-S-H gel, which reduced unfilled pores between particles [15], especially under the SC regime. For instance, the minimum value of 20.08 % at 90d was obtained with a 21% addition of OPC and 50 % replacement of coal fly ash (5S) in comparison to 27.8 % at 90d with a 9% addition of OPC and at constant CFA content of 50 % (1S) with a constant water to binder ratio of 0.28. A decrease in water absorption was within the range of 07%–28%; 05%–17% and 04%–18% (with OPC addition varies at 12%–21%) for 2S to 5S; 7S to 10S and 12S to 15S, respectively as compared to their corresponding first dosages of OPC at 9% (1S, 6S and 11S). Water absorption depends upon pore distribution in the product [45]. Similarly, excessive water absorption is an indication of increased void volume in the product [46]. In addition to C-A-S-H gel, forming pressure also plays a key role in dropping the porosity since the distance between particles decreases; however, excessive pressure should be avoided because of its negative effects [47]. The decrease in water absorption was attributed to the formation of cement hydration products i.e., C–S–H gel developing from a reaction occurring between tri-calcium silicate (C_3S) and di-calcium silicate (C_2S) with water [19]. On the contrary, the water absorption of normal cured specimens followed a similar trend with the addition of cement, however, the values were higher in comparison to the steam-cured specimens at 90d. For instance, the percentage decrease for normal cured specimen in mix designs 2 N–5 N; 7 N–10 N, and 12 N–15 N at 90d was 07%–27 %; 04%–19%, and 03–16% as compared to the first dosage at 9% (1 N, 6 N and 11 N).

The results revealed that water absorption increased with the increase in the replacement of CFA. This is consistent with the available literature [4,12]. This is mainly due to the reason that porosity increases with an increase in the replacement of CFA [8,13]. Moreover, with an increase in the ash content, density decreases while the water absorption varies inversely. So higher density results in lower water absorption and vice versa, since it involves fewer internal ducts and capillary pores, which can hold water [48]. For instance, a mixture design incorporating 50% replacement of CFA (5S) has shown a minimum value of 20.08 % corresponding to an increased value of 23.7 % and 25.5 % with replacement of 60% (10S) and 70 % (15S). Accordingly, the increase in WA varies in the range from 3% to 15% for 6S to 10S and from 10% to 21% for 11S to 15S as compared to the first dosage 1S to 5S. On the contrary, the water absorption of normal cured specimens followed a similar trend with an increase in the replacement of CFA, however, the values are higher in comparison to the steam-cured specimens. For example, the percentage increase for normal cured specimens in mix designs 6 N–10 N; and 11 N–15 N at 90d was 05%–15 % and 10%–22% as compared to the first dosage at 9% (1 N–5 N). It was observed that a mixture design incorporating 9% OPC and 50% CFA (1S) has achieved reduced water absorption i.e. 20.75 % at 28d indicating improved mechanical properties under the influence of steam curing treatment.

Fig. 9 (a) indicates the percentage increase in WA of steam-cured specimens in all the design mixes over normal/moist cured samples at 28d. This effect was supported by various studies that α-dicalcium silicate hydrate with low density and in addition to it,

large voids were formed due to the rapid formation of C–S–H gel that results in non-uniform distribution of gel structure and causes capillary breaks [46]. Further research indicated that C–S–H was loosely packed, and contained porous and large gel pores in the beginning, which become denser, and large gel pores reduced at later ages as the hydration and pozzolanic reactions continue. Moreover, the pastes containing lower w/b ratio; higher replacement volumes of CFA, and subjected to high-temperature curing impede the hydration of cement at an early stage due to insufficient place for C–S–H resulting from cement hydration to growth [49]. Therefore, the water absorption was somewhat higher at a certain age (at the 28d) of the product for steam-cured samples which ranges from 10 to 13%; 9–11%, and 8%–9% in 1S to 5S; 6S to 10S and 11S to 15S. Fig. 9 (b) indicates improvement in the gel structure of the FCB sample in all steam-cured samples. This was due to the micro-cracking caused by the steam curing or uneven distribution of hydration products were ultimately improved/filled by the extended pozzolanic reaction by the FA which also cross-bond with C–S–H at later ages [50]. For instance, the WA values were 02%–2% lower in 1S to 5S: 4% to 2 % lower in 6S to 10S, and 1%–3% lower in 11S to 15S than in NC specimen. Hence, the water absorption values of steam-cured samples decreased as compared to normal-cured samples.

In addition to the current research, the Ordinary Portland Cement (OPC) in this study contains periclase (MgO) contents of 2.80 % which were less than the chemical limit as reported in China, the UK, Canada as 5 %, and in the US 6%. Past research indicated that slow hydration of cement made with higher contents of MgO can result in delayed expansion and cracking. However, cement containing lesser MgO also has a chance to develop cracks and expansion due to C_3A and free CaO to meet ASTM C150 expansion limits.

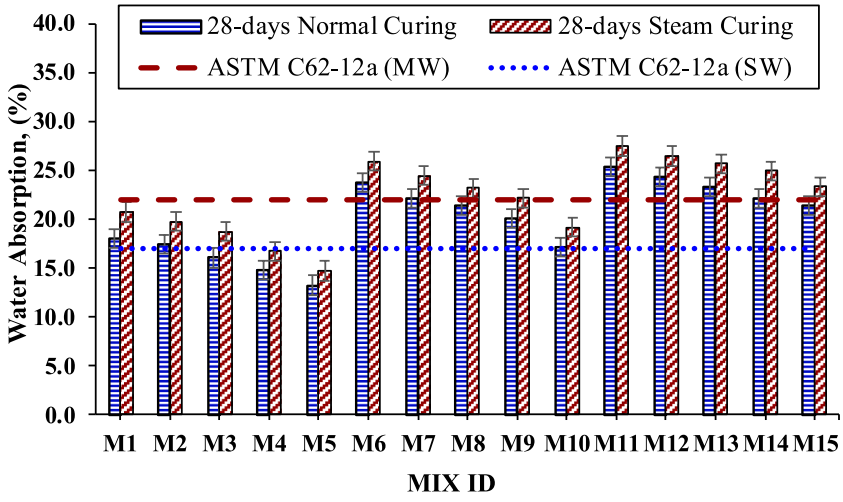

(a)

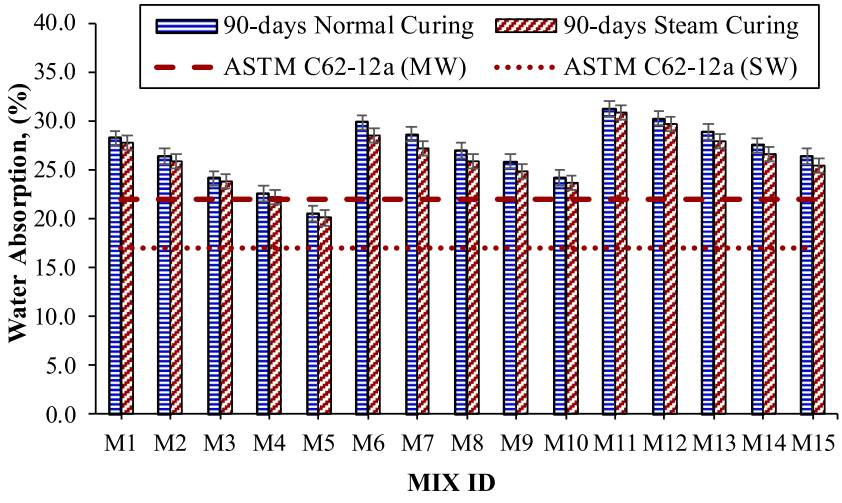

(b)

Fig. 9. Water absorption of main FCB with different OPC and CFA contents under normal and steam curing regime.

So, it is important to check the soundness which does not exhibit the cracking that occurred from volumetric expansion before certain applications of cement. The addition of supplementary cementitious materials as a partial replacement of cement may also play a significant role in volume stability as highlighted by previous research. Hence, performance/expansion evaluation through the Le Chatelier test or ASTM autoclave expansion of Portland cement (ASTM C151) due to delayed MgO hydration and free CaO is opined for further research [51,52].

Moreover, results of water absorption involving various quantities of CFA and OPC were also compared with limiting values as specified by ASTM C62-12a (SW) and (MW) i.e., 17% and 22%, respectively. Mixture designs incorporating 21% OPC and 50% CFA content (5S, 5 N) have satisfied limiting values of ASTM C62-12a (MW) at 90d.

4.4.1.6. Initial rate of water absorption (influence on addition of OPC, replacement of CFA, and different curing regimes). Fig. 10 depicts the effect of the dosage of OPC and replacement of CFA, curing regimes on the IRWA of FCB specimen. The average results of five FCB under NC and SC cured specimens were assessed at the curing age of 28d and 90d. Table 4 shows the coefficient of variation (CoV) of the initial rate of water absorption for all the mixture designs was less than 1%. The trend of IRWA was similar to that of water absorption [4]. The initial rate of water absorption is typically a measure of the bond between bricks and mortar. Higher value results in too early drying of brick weakens the mortar, and hence, reduces its adherence to brick [53]. With the increase in the replacement of OPC with CFA, the initial rate of water absorption was reduced in both regimes probably due to the formation of C-A-S-H gel, which

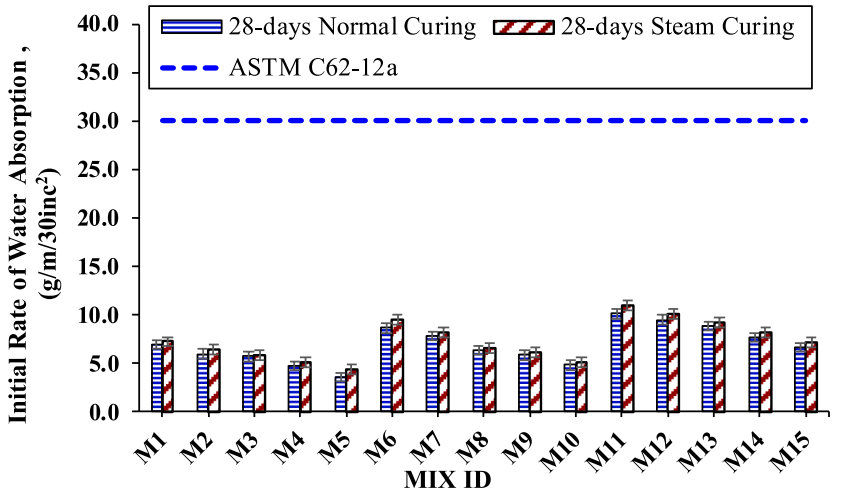

(a)

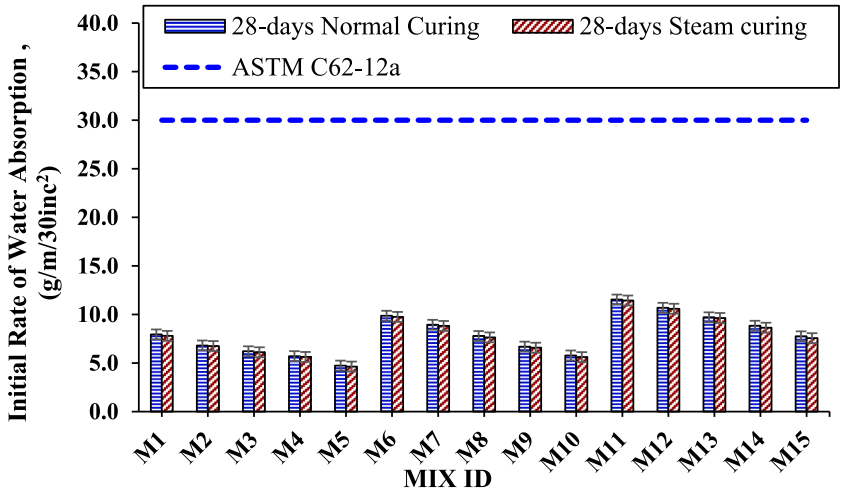

(b)

Fig. 10. Initial Rate of Water Absorption of Main FCB with different OPC and CFA contents under Normal and Steam Curing Regime.

reduced unfilled pores between particles [15], especially under the SC regime. For instance, minimum value of 4.64 g/min per 30 in^2 at 90d was obtained with 21% addition of OPC and 50 % replacement of coal fly ash (5S) in comparison to 7.8 g/min per 30 in^2 at 90d with 9% addition of OPC and at constant CFA content of 50 % (1S) with a constant water to binder ratio of 0.28. A decrease in the initial rate of water absorption was within the range of 13%–41%; 10%–42% and 07%–34% (with OPC addition varying from 12% to 21%) for 2S to 5S; 7S to 10S and 12S to 15S, respectively as compared to their corresponding first dosages of OPC at 9% (1S, 6S and 11S). On the contrary, the initial rate of water absorption of normal cured specimens follows a similar trend with an increase in the addition of cement, however, the values are higher in comparison to the steam-cured specimens at 90d. For instance, the percentage decrease for normal cured specimen in mix designs 2 N–5 N; 7 N–10 N, and 12 N–15 N at 90d was 14%–40%; 09%–41%, and 07–33% as compared to the first dosage at 9% (1 N, 6 N and 11 N).

The results showed that the initial rate of water absorption increased with an increase in the replacement of CFA. This was consistent with the available literature [4]. This is mainly due to the reason that porosity increases with an increase in the replacement of cement with CFA [10,13]. Moreover, with an increase in the ash content, density decreases while the initial rate of water absorption varies inversely. So, higher density results in a lower initial rate of water absorption and vice versa, since it involves fewer internal ducts and capillary pores, which can hold water [48]. For example, a mixture design incorporating 50% replacement of CFA (5S) has shown a minimum value of 4.64 g/min per 30 in^2 corresponding to an increased value of 5.61 g/min per 30 in^2 and 7.56 g/min per 30 in^2 with replacement of 60% (10S) and 70 % (15S). Accordingly, the increase in IRWA varies in the range from 25% to 21% for 6S to 10S and from 47% to 63% for 11S to 15S as compared to the first dosage 1S to 5S. Conversely, the initial rate of water absorption of normal-cured specimens followed a similar trend with an increase in replacement of CFA, however, the values were higher in comparison to steam-cured specimens at 90d. For example, the percentage increase for normal cured specimens in mix designs 6 N–10 N; and 11 N–15 N at 90d was 20% to 17 % and 45%–64% as compared to the first dosage at 9% (1 N–5 N).

Fig. 10(a) indicates the percentage increase in IRWA of steam-cured samples in all the design mixes over normal/moist-cured samples at 28d. This effect was supported by various studies that α-dicalcium silicate hydrate with low density and large voids are formed due to the rapid formation of C–S–H gel that results in non-uniform distribution of gel structure and causes capillary breaks [46]. Extra CSH gel formation has a filler effect and helps in reducing the initial rate of water absorption. Therefore, the initial rate of water absorption values was somewhat higher for a certain age (at 28d) of the product which ranges from 04 to 18%; 09 to 05%, and 08 to 07% in 1S to 5S; 6S to 10S, and 11S to 15S. Fig. 10 (b) indicates improvement in the gel structure of the FCB sample in all steam-cured samples. This might be due to the micro-cracking caused by the steam curing or uneven distribution of hydration products that were ultimately improved/filled by the pozzolanic reaction by the FA which also cross-bond with C–S–H at later ages [50]. Hence, the initial rate of water absorption values of steam-cured samples decreased as compared to normal-cured samples. For instance, the IRWA values are 02%–2% lower in 1S to 5S; 1% to 3 % lower in 6S to 10S, and 1%–2% lower in 11S to 15S than the NC specimen.

Moreover, results of the initial rate of water absorption involving various quantities of CFA and OPC were also compared with limiting values as specified by ASTM C62-12a i.e. 30 g/min per 30 in^2. IRWA values of all mix designs satisfied the limiting value of ASTM C62-12a (MW) at 28d and 90d.

4.4.1.7. Efflorescence. Fig. 11 shows the results of FCB specimens related to efflorescence under NC and SC curing regimes at 28d and 90d. The results revealed that neither FCB specimen under SC at 28d showed efflorescence marks nor at 90d and those FCB specimens were reported as "NIL or 0" as per ASTM C 67-05. It was observed that the pozzolanic reaction prevented efflorescence apart from strength contribution [9]. Moreover, fewer FCB specimens under NC had shown efflorescence and those were reported as "Effloresced or 1" which was due to the presence of free lime [14]. For instance, mixture designs incorporating the 21% OPC and 70% CFA had shown efflorescence at 28d and 90d, due to the presence of free lime content in it.

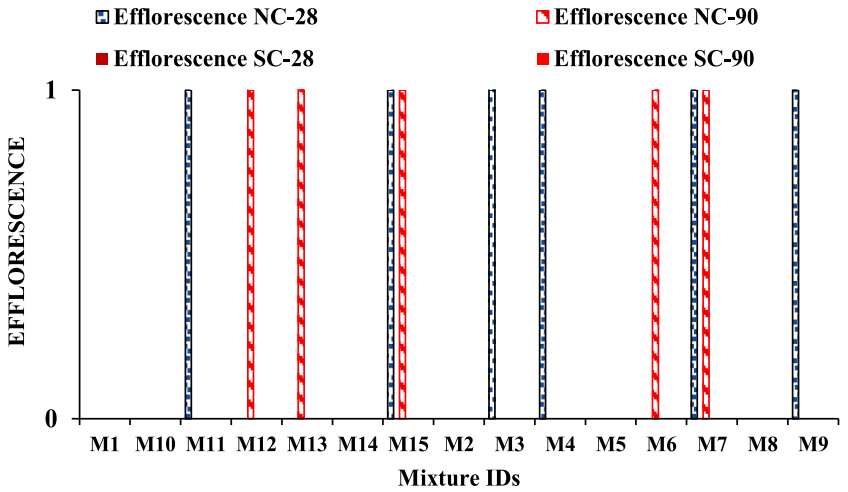

Fig. 11. Efflorescence of Main FCB with different OPC and CFA contents under Normal and Steam Curing Regime.

4.4.1.8. Cost Comparison. Fig. 12 depicts the cost comparison of Burnt Clay Brick (BCB), and unburnt coal ash brick (UCAB) with FCB specimens under NC and SC conditions. It has been observed that due to price escalation in the cost of raw materials and higher electricity cost per unit, the per unit cost of FCB was somewhat higher than BCB cost and UCAB cost i.e. PKR 12.3 per unit as evaluated by Qazi et al. (2022) with 15 % cement contents. The cost of FCB samples under SC conditions is a bit higher than NC conditions due to additional cost involved for steam curing arrangements i.e., electricity cost. For instance, 5S has a maximum cost of PKR 16.76 whereas 5 N has a cost of PKR 13.70, which is less than BCB cost.

4.5. Micromorphology of FCB specimen

Fig. 13 shows the micromorphology/SEM analysis of the FCB specimen under the NC and SC conditions. Fig. 13 (a) depicts SEM images of MD under NC (5 N). It indicates the amorphous irregular structure of CFA (most of the unreacted minerals of CFA which did not undergo melting) with traces of C–S–H formulation. Fig. 13 (b) indicates SEM images of MD results under SC conditions (5S) indicate less uniform distribution of hydration products or gapped/porous structure/high micro-cracking along with excessive C–S–H gel formation. Accelerated hydration of cement under steam curing and the early generation of CH provides a medium for extended pozzolanic reactions (EPR), the gel generated by EPR of CFA not only filled the pores but cross-bond with C–S–H and C-A-S-H which increase the overall strength of gel system and improves the microstructure solidity [50,54]. This in turn decreases the thermal damage caused by steam curing. Fig. 13 (c) indicates SEM images of mixture design results under NC conditions (11 N); most of the cloudy structure includes the amorphous irregular structure of CFA and lesser C–S–H formation. Fig. 13 (d) indicates SEM images of mixture design results under SC conditions (11S); less uniform distribution of hydration products or gapped/porous structure with slight C–S–H formation. Steam curing enhanced the hydration of cement, forming a pore solution, and facilitating the pozzolanic reaction between fly ash and portlandite, creating C-A-S-H. The detrimental effects of heat treatment of FCB specimens improved through the long-lasting formation of C-A-S-H by pozzolanic reaction since large substitution of CFA needs a long time for curing. Whereas, the presence of un-hydrated carbon fragments weakens the structure. The irregular and amorphous structure of CFA may be due to un-burnt carbon, anhydrate, and calcite [8].

4.6. Energy dispersive X-ray analysis of FCB specimen

Fig. 14 shows the results of energy dispersive X-ray analysis of the main FCB under NC and SC regimes. The major peaks of calcium, silicon, carbon, and iron contents were observed. The results so obtained were consistent with the chemical composition of materials of the main FCB.

5. Conclusions and recommendations

This study was intended to produce eco-friendly and sustainable production of fly ash-cement sand composite brick through the reduction and appropriate application of coal fly ash. This study evaluated the use of high volume utilization of fly ash with 50%, 60%, and 70% contents, cement addition of 9%, 12%, 15%, 18%, and 21% along with stone dust and sand contents. Trial waste coal ash brick under normal/moist curing exhibited delayed strength, which was the prime focus and to limit the same during this course of research through the development of FCB with the application of effective steam curing treatment.

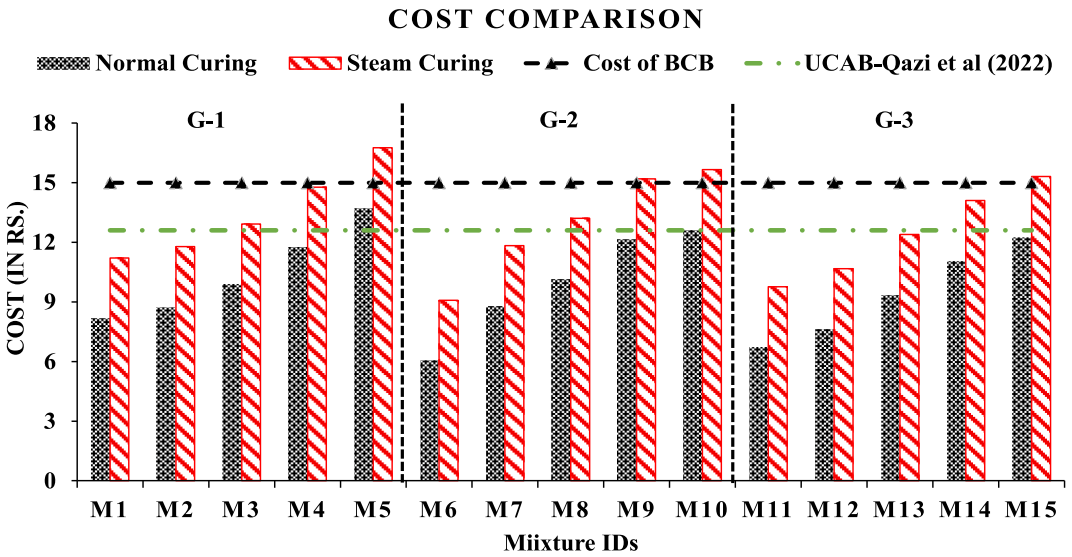

Fig. 12. Cost Comparison of main FCB (under NC and SC regimes) with BCB and UCAB.

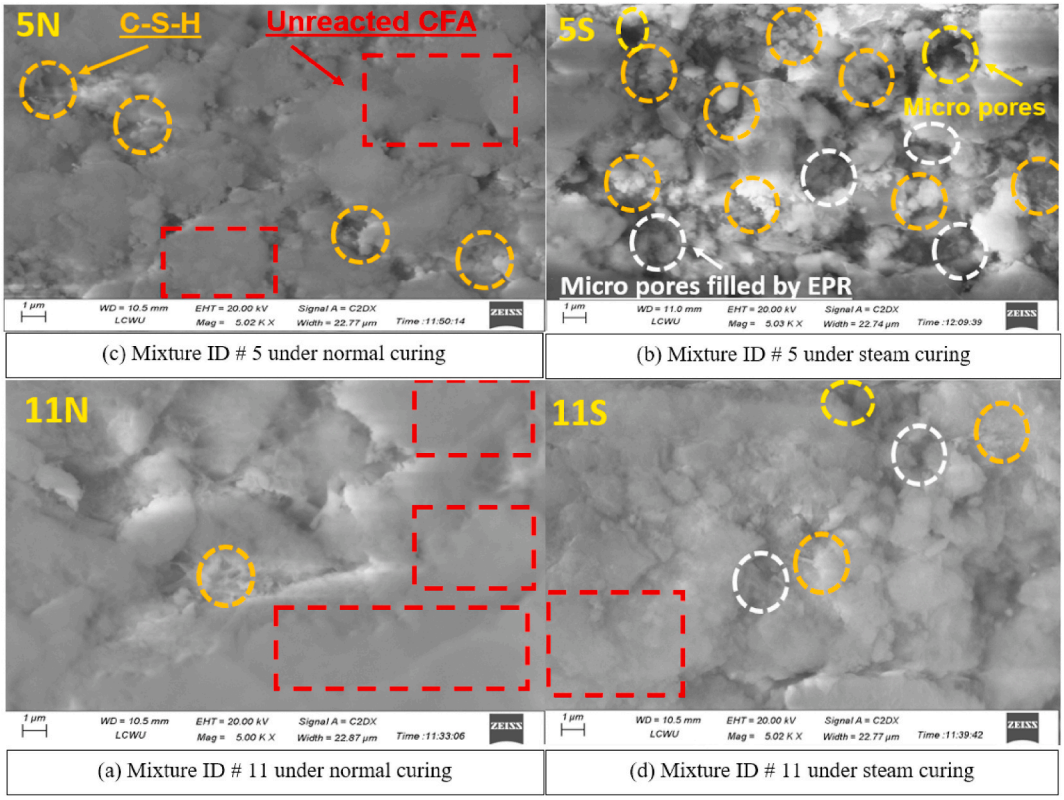

Fig. 13. Scanning Electron Microscopy analysis of main FCB.

1. Steam curing significantly enhances the physical, mechanical, and durability properties of fly ash-cement sand composite bricks (FCB) compared to normal curing. The compressive strength of the main FCB, utilizing the mix design MD (9:50:37:4), yielded 4.95 MPa at 28 days. Other durability properties also showed improved performance with steam curing.
2. An optimized mix design, MD: 5S (21:50:26:3), outperformed and achieved a compressive strength of 15.57 MPa, flexural strength of 0.67 MPa, a water absorption rate of 20.08%, and an initial rate of water absorption of 4.64 g/min per 30 in^2, with no efflorescence observed.
3. Microstructural analysis revealed that although steam curing temporarily weakened specimens the final product benefited from an enriched structure formed by an extended pozzolanic reaction.
4. Cost comparison indicates that SC results showed appreciable results over normal curing (NC) Notably, mix design #6 (9:60:28:3) proved to be the most cost-effective option, whereas mix design #5 (21:50:26:3), due to higher cement content, incurred higher costs, albeit still competitive with other board types.

In conclusion, it is imperative to avoid excessive CFA replacement beyond 50% in FCB specimens, even with steam curing, as it compromises early-age strength and durability properties. Future endeavors should explore the industrial potential of steam curing setups, particularly in challenging weather conditions like winter and also investigate about unsoundness of the main FCB despite having low periclase content. Additionally, the incorporation of finer admixtures warrants further investigation to enhance FCB performance.

Data availability statement

All the relevant data has been presented in the manuscript.

CRediT authorship contribution statement

Wasim Abbass: Writing – original draft, Conceptualization. **Soheeb Ullah Mahmood:** Investigation, Formal analysis, Data curation. **Ali Ahmed:** Supervision, Investigation, Formal analysis. **Fahid Aslam:** Writing – review & editing, Validation, Software, Conceptualization. **Abdullah Mohamed:** Writing – review & editing, Visualization, Validation, Supervision.

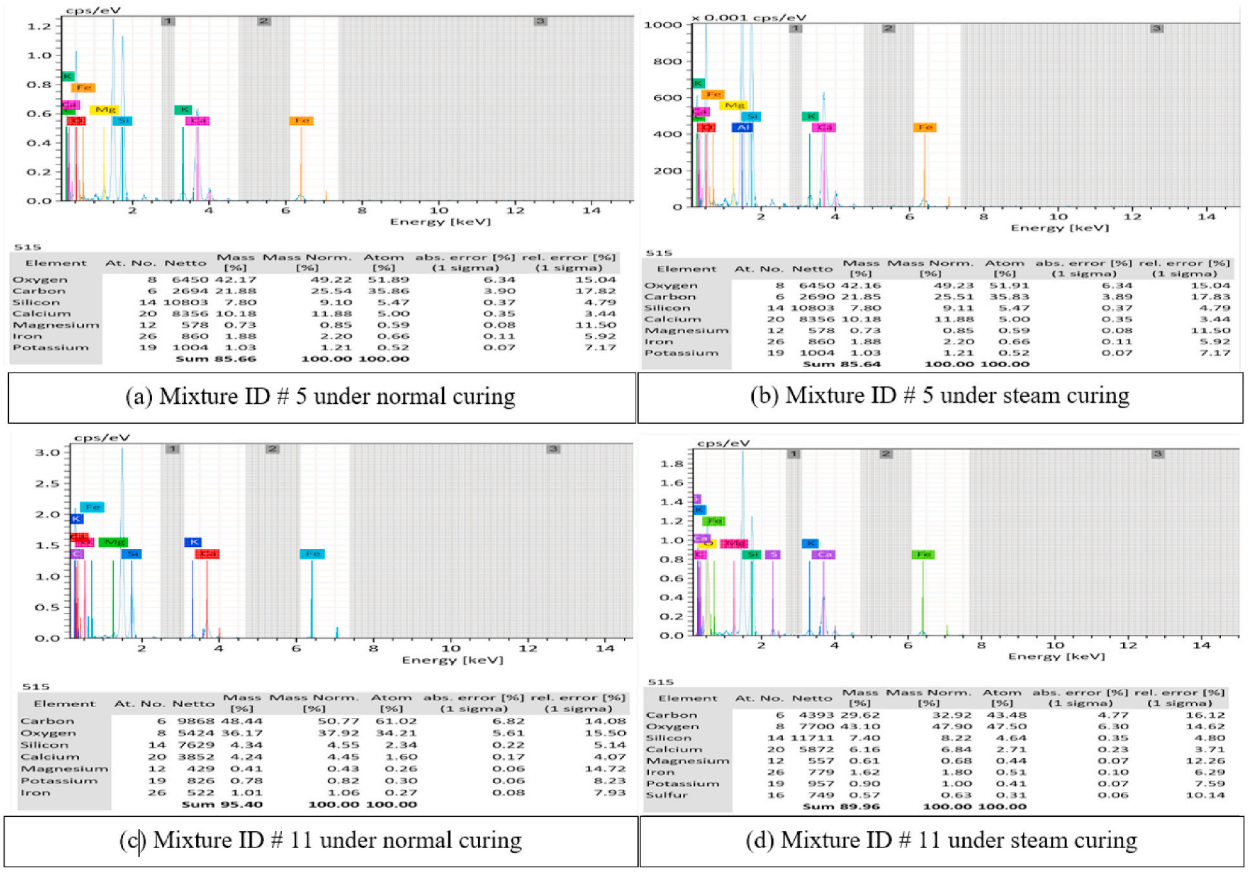

Fig. 14. Energy dispersive X-ray analysis of main FCB.

Declaration of competing interest

The authors declare that they have no known competing financial interests or personal relationships that could have appeared to influence the work reported in this paper.

Acknowledgment

This study is partially funded by the Future University in Egypt (FUE).

The authors of this work pay special thanks to faculty members of the Civil Engineering Department, UET Lahore for their guidance and technical support for this research work and are thankful to laboratory staff for their assistance in experimental arrangements.

This study is supported via funding from Prince Sattam bin Abdulaziz University project number (PSAU/2024/R/1445)

References

[1] S. Shaikh, A.A. Nafees, V. Khetpal, Respiratory Systems and Illness Among Brick Kiln Workers: a Cross Sectional Study from Rural Districts of Punjab, Article in BMC Public Health, November 2012, https://doi.org/10.1186/1471-2458-12-999.

[2] M.W. Khan, Y. Ali, Impacts of brick kilns industry on environment and human health in Pakistan 2019, Sci. Total Environ. 678 (2019) 383–389, https://doi.org/10.1016/j.scitotenv.2019.04.369.

[3] Fact sheet brick sector in Pakistan, Available online: https://www.ccacoalition.org/en/resources/fact-sheet-brick-sector-pakistan. (accessed on 31.July.2023).

[4] W. Abbass, S. Abbas, F. Aslam, A. Ahmad, Manufacturing of sustainable untreated coal ash masonry units for structural applications, Materials 15 (2022) 4003, https://doi.org/10.3390/ma15114003.

[5] A. Shetkar, N. Hanche, Experimental Studies on fly ash based lime bricks, International Journal of Recent Advances in Engineering & Technology (IJRAET) 4 (7) (2016). ISSN (Online): 2347 - 2812.

[6] Economic Survey of Pakistan 2021-22, Available online: https://www.finance.gov.pk/survey/chapter_22/PES14-ENERGY.pdf. (accessed on 31.July.2023).

[7] A.S. More, A. Tarade, Assessment of suitability of fly ash and Rice Husk ash burnt clay bricks, International Journal of Scientific and Research Publications 4 (Issue 7) (July 2014 1). ISSN 2250-3153.

[8] Z.T. Yao, X.S. Ji, A comprehensive review on the applications of coal fly ash, Earth Sci. Rev. 141 (2015) 105–121, https://doi.org/10.1016/j.earscirev.2014.11.016.

[9] Gamage N.; Liyanage K. Overview of Different Types of Fly Ash and their Use as a Building and Construction Material, http://dl.lib.mrt.ac.lk/handle/123/9367.

[10] A. Kumar, R. Kumar, Assessing the structural efficiency and durability of burnt clay bricks incorporating fly ash and silica fume as additives, Construct. Build. Mater. 310 (2021) 125233, https://doi.org/10.1016/j.conbuildmat.2021.125233. Available online 20 October 2021.
[11] D. Eliche-Quesada, J. Leite-Costa, Use of Bottom Ash from olive pomace combustion in the production of eco-friendly fired clay bricks, Waste Manag. 48 (2016) 323–333, https://doi.org/10.1016/j.wasman.2015.11.042.
[12] G.L. Golewski, Examination of water absorption of low volume fly Ash Concrete (LVFAC) under water immersion conditions, Mater. Res. Express 10 (8) (2023) 085505, https://doi.org/10.1088/2053-1591/acedef.
[13] G.L. Golewski, Assessing of water absorption on concrete composites containing fly ash up to 30 % in regard to structures completely immersed in water, Case Stud. Constr. Mater. 19 (2023), https://doi.org/10.1016/j.cscm.2023.e02337.
[14] A. Mukhtar, A.U. Qazi, Q.S. Khan, Feasibility of using coal ash for the production of sustainable bricks, Sustainability 14 (2022) 6692, https://doi.org/10.3390/su14116692.
[15] Ahmad M.; Rashid K. Physico-mechanical performance of fly ash based geopolymer brick: Influence of pressure - temperature – time. J. Build. Eng. 50 (2022) 104161. Available online 3 February 2022. https://doi.org/10.1016/j.jobe.2022.104161..
[16] A.M. Zeyad, B.A. Tayeh, A. Adesina, Review on effect of steam curing on behavior of concrete, Cleaner Materials 3 (2022) 100042, https://doi.org/10.1016/j.clema.2022.100042.
[17] Q. Yang, S. Zhang, S. Huang, Effect of ground quartz sand on properties of high-strength concrete in the steam-autoclaved curing, Cement Concr. Res. 30 (2000) 1993–1998, https://doi.org/10.1016/S0008-8846(00)00395-1.
[18] T. Çiçek, Y. Çinçin, Use of fly ash in production of light-weight building bricks, Construct. Build. Mater. 94 (2015) 521–527, https://doi.org/10.1016/j.conbuildmat.2015.07.029.
[19] Mindess S.; Young J. F.; Darwin D. Concrete, second ed., Chapter: 12, Section 12.2, Curing at Elevated Temperatures..
[20] S. Maitra, S. Das, A. Basumajumdar, Effect of heat treatment on properties of steam cured fly ash–lime compacts, Bull. Mater. Sci. (December 2005), https://doi.org/10.1007/BF02708540.
[21] V.M. Tran, L.T. Nguyen, T.H.Y. Nguyen, Enhancing the effectiveness of steam curing for cement paste incorporating fly ash based on long-term compressive strength and reaction degree of fly ash, Case Stud. Constr. Mater. 16 (2022) e01146, https://doi.org/10.1016/j.cscm.2022.e01146. Available online 11 May 2022.
[22] W. Zhen-Shaung, Influence of fly ash on the mechanical properties of frame concrete, Sustain. Cities Soc. 1 (2011) 164–169, https://doi.org/10.1016/j.scs.2011.06.001.
[23] H. Yazici, Effect of Steam Curing on Class C High-Volume Fly Ash Concrete Mixtures, 2004.
[24] R.A. Khan, J.N. Akhtar, R.A. Khan, Experimental study on fine-crushed stone dust a solid waste as a partial replacement of cement, In Press. Available online, https://doi.org/10.1016/j.matpr.2023.03.222, 2023.
[25] A.A.M. Ahmed, H.M.A. Mahzuz, Minimizing the stone dust through a sustainable way: a case study of stone crushing industry of Sylhet, Proc. of International Conference on Environmental Aspects of Bangladesh (ICEAB10), Japan (Sept. 2010), https://doi.org/10.13140/2.1.2012.7041.
[26] Junaid M.T.; Khennane A.; Kayali O. Performance of fly ash based geopolymer concrete made using non-pelletized fly ash aggregates after exposure to high temperatures, Mater. Struct. 48 3357–3365, https://doi.org/10.1617/s11527-014-0404-6..
[27] R. Yadav, P.K. Kushwaha, M.K. Rana, Effect of waste Glass powder and stone dust on the characteristics of concrete, Int. J. Res. Appl. Sci. Eng. Technol. 9 (I) (Jan 2021). ISSN: 2321-9653; IC Value: 45.98, https://www.ijraset.com/fileserve.php?FID=32826.
[28] G. Turuallo, H. Mallisa, N. Rupang, Sustainable development: using stone dust to replace a part of sand in concrete mixture, MATEC Web of Conferences 331 (2020) 05001, https://doi.org/10.1051/matecconf/202033105001.
[29] Y. Chen, Y. Zhang, Preparation of eco-friendly construction bricks from hematite tailings, Construct. Build. Mater. 25 (2011) 2107–2111, https://doi.org/10.1016/j.conbuildmat.2010.11.025.
[30] ASTM C618-12a, Standard Specification for Coal Fly Ash and Raw or Calcined Natural Pozzolan for Use in Concrete, ASTM International, PA, USA, 2014.
[31] ASTM C136-06; Standard Test Method for Sieve Analysis of Fine and Coarse Aggregates. ASTM International: PA, USA..
[32] ASTM C67-05 Standard Test Methods for Sampling and Testing Brick and Structural Clay Tile. ASTM International: PA, USA.
[33] PBC, Pakistan Building Code-Seismic Provisions, Pakistan Engineering Council, Islamabad, Pakistan, 2007.
[34] ASTM C62-12a Standard Specification for Building Brick (Solid Masonry Units Made from Clay or Shale). ASTM International: PA, USA.
[35] A.A. Abdalla, et al., Microstructure, Chemical Compositions, and Soft Computing Models to Evaluate the Influence of Silicon Dioxide and Calcium Oxide on the Compressive Strength of Cement Mortar Modified with Cement Kiln Dust, 2022.
[36] A. Abdulmatin, W. Tangchirapat, C. Jaturaptakkul, An investigation of bottom ash as a pozzolanic material, Construct. Build. Mater. 186 (2018) 155–162.
[37] A. Chajec, A. Chowaniec, A. Krolicka, Engineering of green cementitious composites modified with siliceous fly ash: understanding the importance of curing conditions, Construct. Build. Mater. 313 (2021) 125209, https://doi.org/10.1016/j.conbuildmat.2021.125209.
[38] Z. Wu, C. Shi, W. He, Comparative study on flexural properties of ultra-high performance concrete with supplementary cementitious materials under different curing regimes, Construct. Build. Mater. 136 (2017) 307–313, https://doi.org/10.1016/j.conbuildmat.2017.01.052.
[39] W. Guo, Q. Zhao, Y. Sun, Effects of various curing methods on the compressive strength and microstructure of blast furnace slag-fly ash based cementitious material activated by alkaline solid wastes, Construct. Build. Mater. 357 (2022) 129397, https://doi.org/10.1016/j.conbuildmat.2022.129397.
[40] C.S. Poon, L. Lam, Y.L. Wong, A study on high strength concrete prepared with large volumes of low calcium fly ash, Cement Concr. Res. 30 (2000) 447–455, https://doi.org/10.1016/S0008-8846(99)00271-9.
[41] S. Kumar, et al., Fly Ash–Lime–Phosphogypsum Hollow Blocks for Walls and Partitions, 2003.
[42] Z. Zuo, J. Zhang, B. Li, X. Chen, Effect of curing regime on the mechanical strength, hydration and microstructure of ecological ultra-high performance concrete (EUHPC), Materials 15 (2022) 1668, https://doi.org/10.3390/ma15051668.
[43] A. Shanmugasundaram, K. Jayakumar, Effect of curing regimes on microstructural and strength characteristics of UHPC with ultra-fine fly ash and ultra-fine slag as a replacement for silica fume, Arabian J. Geosci. 15 (2022) 345, https://doi.org/10.1007/s12517-022-09617-y.
[44] H. Yazıcı, the effect of curing conditions on compressive strength of ultra-high strength concrete with high volume mineral admixtures, Build. Environ. 42 (2007) 2083–2089, https://doi.org/10.1016/j.buildenv.2006.03.013.
[45] S. Aprana, D. Sathyan, Microstructural and rate of water absorption on fly-ash incorporated cement mortar, Mater. Today: Proc. 5 (2018) 23692–23701, https://doi.org/10.1016/j.matpr.2018.10.159.
[46] Mardani-Aghabaglou A.; Özen S. Effect of curing conditions during the first 24 hours after casting on the properties of mortar mixtures, Manuscript Code: 1471. DOI: 10.7764/RDLC.19.1.68-79..
[47] J.M. Pérez, M. Romero, Microstructure and technological properties of porcelain stoneware tiles moulded at different pressures and thicknesses, Ceram. Int. 40 (2014) 1365–1377, https://doi.org/10.1016/j.ceramint.2013.07.018.
[48] C. Leiva, C. Arenas, B. Alonso-fariñas, L.F. Vilches, Characteristics of fired bricks with co-combustion fly ashes, J. Build. Eng. 5 (2016) 114–118, https://doi.org/10.1016/j.jobe.2015.12.001.
[49] M. Narmluk, T. Nawa, Effect of fly ash on the kinetics of Portland cement hydration at different curing temperatures, Cement Concr. Res. 41 (2011) 579–589, https://doi.org/10.1016/j.cemconres.2011.02.005.
[50] Y. Duan, Q. Wang, Investigating the impact of fly ash on the strength and micro-structure of concrete during steam curing and subsequent stages, Materials 16 (2023) 1326, https://doi.org/10.3390/ma16041326.
[51] H. Kabir, R.D. Hooton, Evaluation of cement soundness using the ASTM C151 autoclave expansion, Cement Concr. Res. 136 (2020) 106159, https://doi.org/10.1016/j.cemconres.2020.106159.

[52] P.K. Mehta, History and status of performance tests for evaluation of soundness of cements, in: Cement Standards—Evolution and Trends, ASTM International, 1978, https://doi.org/10.1520/STP35785S, 1978.
[53] O. Kayali, High performance bricks from fly ash, World of Coal Ash (WOCA), Lexington, Kentucky, USA, 2005.
[54] S. Singh, G.D. Ransinchung, P. Kumar, Effect of mineral admixtures on fresh, mechanical and durability properties of RAP inclusive concrete, Construct. Build. Mater. 156 (2017) 19–27, https://doi.org/10.1016/j.conbuildmat.2017.08.144.